RSC Advances

ROYAL SOCIETY OF CHEMISTRY

www.rsc.org/advances

Investigation of the Nonlinear Absorption Spectrum of All-Trans Retinoic Acid by Using the Steady and Transient Two-Photon Absorption Spectroscopy

M.G. Vivas[1,2*], J. P. Siqueira[1], D. L. Silva[3], L. De Boni[1] and C. R. Mendonca[1,*]

[1]*Instituto de Física de São Carlos, Universidade de São Paulo, Caixa Postal 369, 13560-970 São Carlos, SP*

[2]*Instituto de Ciência de Tecnologia, Universidade Federal de Alfenas, Cidade Universitária - BR 267 Km 533, 37715-400 Poços de Caldas, MG, Brazil*

[3]*Departamento de Ciências da Natureza, Matemática e Educação, Universidade Federal de São Carlos, Rod. Anhanguera – Km 174,13600-970 Araras, SP, Brazil*

**Corresponding Author: mavivas82@gmail.com and crmendon@ifsc.usp.br*

Abstract: This work investigates the two-photon absorption (2PA) spectrum of all-trans retinoic acid (**ATRA**) in DMSO solution, employing the wavelength-tunable Z-scan and white-light pump-probe techniques with femtosecond pulses. Our results showed that **ATRA** presents two 2PA allowed bands at 280 nm (2 hν = 560 nm) and 365 nm (2 hν = 730 nm) with 2PA cross-section values of 34 GM and 40 GM, respectively. The 2PA band at 280 nm was ascribed to the transition from ground to high energy excited states with contribution of the real intermediate excited state ($1^1B_u^+$-like). The 2PA band at 365 nm was attributed to an overlap of $1^1B_u^+$-like and 2^1Ag^- -like excited states, which are essential to describe the photochemical processes that this class of organic materials play in nature. Through solvatochromic measurements and by using the two-energy level approach, we found that the $1^1B_u^+$-like and 2^1Ag^- -like states contribute, respectively, with 48 % and 52 % of the lowest energy 2PA band of **ATRA** in DMSO solution. From femtosecond transient spectroscopy we verified that when **ATRA** is excited at 775 nm (2PA excitation) its excited state absorption (ESA) spectrum presents a red-shift of ~5.5 nm in comparison to the same spectrum excited at 387.5 nm (1PA excitation), corroborating the interpretation about the 2PA spectrum for the **ATRA** in DMSO.

I - INTRODUCTION

Organic compounds with biological relevance such as retinoids, carotenoids and flavonoids have emerged as potential candidates for applications in bio-photonic devices due to their capacity to convert optical signals into biochemical events, serving as ultrafast electro-optical devices [1-5]. For instance, carotenoids act as light-harvesting pigments and efficiently transfer energy to bacteriochlorophyll[6-8]; flavonoids, due to their antioxidant activity, have been used for the development of biological and pharmaceutical products [9-11] and retinal molecules are key chromophores found in the opsin [12, 13], being responsible for visible light absorption and subsequent conversion into nervous impulses via photoisomerization [14-18].

Among the retinyl polyenes, the all-trans retinoic acid (**ATRA**) has been the least studied from the photophysical and nonlinear optical response points of view. However, **ATRA** presents important biological functions, such as the activating gene transcription through their chemical binding to heterodimers of the retinoic acid receptor (RAR) [19]. Nevertheless, retinyl polyenes, in general, are almost insoluble and chemically unstable in the aqueous medium [20]. Consequently, **ATRA** is found bound to specific retinoid-binding proteins to be protected and transported in body fluids [21]. On the other hand, in polar organic solvents like dimethyl sulfoxide (DMSO) and ethanol, it presents high solubility and good chemical stability [22]. As it can be seen in Fig. 1, the **ATRA** has five C=C double bonds in its polyene backbone connected by a carboxylic acid and a β-ionone group in its extremities (linear structure); a structural analogue of carotenoids with a fewer number of conjugated C=C bonds.

Retinyl polyenes are well-known because of their biological role and, therefore, they have been the subject of numerous theoretical and spectroscopic studies in the last decades. One of the first studies in this class of materials using two-photon absorption (2PA) excitation was performed by Birge et. al. [23, 24], using fluorescence technique with nanosecond pulses. According to that study, the all-trans retinal (ATR), analogous to the **ATRA**, presents three low-lying excited singlet states with nπ* (1PA allowed weakly), $2^1A_g^-$-like (ππ* - 2PA allowed strongly) and $1^1B_u^+$-like (ππ* - 1PA allowed strongly) symmetries, respectively. It is important to mention that the $2^1A_g^-$ state is forbidden by 1PA excitation due to the dipole electric selection rules, since retinyl polyenes derivatives present ground state with $1^1A_g^-$ symmetry [24, 25]. Therefore, to describe the origin and order of these low-lying states in retinyl polyenes, Birge et al. [23, 24] compared the 2PA spectrum for the ATR dissolved in ethyl ether-

isopentane-alcohol (EPA) at 77 K with their one-photon absorption (1PA) spectrum and found a red-shift of ~2800 cm^{-1}. The authors attributed this result to the presence of a two-photon allowed state near to the $1^1B_u^+$-like state. Based on quantum chemical calculations [24], the authors concluded that this state should have the $2^1A_g^-$-like symmetry. Forbidden states like the $2^1A_g^-$like in ATR are extremely important to describe the photochemical properties of these molecules [12]. In this same context and more recently, Yamaguchi and Tahara [26] have employed femtosecond pump-probe technique to measure the 2PA spectrum of ATR in hexane at room temperature. It was also observed a red-shift (~ 7 nm) in the 2PA peak with respect to the one-photon absorption, which also was attributed to presence of $2^1A_g^-$-like state.

Regarding to the **ATRA**, although some works have been published on their photophysical properties, we must mention the recent work of Presiado et. al. [27]. They measured the time-resolved fluorescence spectra dynamics of **ATRA** in several solvents using femtosecond pulses at 390 nm as excitation. They showed that the time-resolved emission signal is composed of three decay components, arising from three different excited-states. They attributed the ultrafast component (80 fs), dominant at $\lambda \leq 500$ nm, to the $1^1B_u^+$-like$\rightarrow 2^1A_g^-$ -like relaxation, while the intermediate component (from 1 to 4 ps, dominant at longer wavelengths) was ascribed to forbidden transition from the excited $2^1A_g^-$ -like state to the ground-state. Another interesting study about the excited state dynamics for the **ATRA** was performed by Lei Zhang, et. al [28]. In that work, they investigated the excited state dynamics of **ATRA** in hexanol purged with Ar with excitation at 400 nm by using the femtosecond time-resolved difference absorption spectroscopy. The authors used the single value decomposition (SVD) method together with global fitting to decompose the excited state absorption spectra and found three fast components, which, according to them, are associated with the S_1 ($2^1A_g^-$), S_2 ($n\pi^*$) and S_3 ($1^1B_u^+$) states. However, both studies were performed employing 1PA excitation that is responsible to populate only the strongly 1PA allowed excited state ($1^1B_u^+$-like). Therefore, a complete study about the transient excited state dynamics induced by 2PA, as well as the 2PA cross-section spectrum for **ATRA** has not been carried out so far, to best of our knowledge.

Nowadays, there are yet a great interest on the low-lying excited states of carotenoids and linear polyenes like **ATRA** [29, 30] due to its relevance in some biological functions. In this context, the aim of this present study is contribute to the better understanding about the photochemical and nonlinear optical properties of **ATRA**. For that, we investigated its degenerate 2PA spectrum in DMSO, using the wavelength tunable femtosecond Z-scan

technique. In an effort to further comprehend the nonlinear spectrum, we carried out femtosecond transient absorption and solvatochromic shift measurements.

II. EXPERIMENTAL

A – LINEAR OPTICAL MEASUREMENTS:

For the ground-state absorption, Stokes-shift and excitation anisotropy measurements, **ATRA** was dissolved in different solvents (toluene, chloroform, THF, DMSO, ethanol) in a concentration of ~1.0×10^{-5}Mol/L. In these experiments, the samples were placed in 1 cm thick quartz cuvette. The steady-state absorption and fluorescence spectra were recorded using a Shimadzu UV-1800 spectrophotometer and a Perkin Elmer LS55 fluorimeter, respectively. ATAR were purchased from Sigma-Aldrich in powder with purity >98%. Linear and nonlinear optical measurements were performed at a temperature of 20^{o}C. We measured the linear absorption and fluorescence spectra before and after each nonlinear optical measurement and no degradation was observed for the temperatures and intensities used.

B – Z-SCAN EXPERIMENTS:

The 2PA cross-section spectra were measured using the Z-scan technique in the open-aperture configuration. The Z-scan measurements were performed with 160-fs pulses at 1 kHz repetition rate, delivered by a tunable optical parametric amplifier pumped at 775 nm by a Ti:Sapphire chirped pulse amplifier (CPA). For each wavelength, the pulse energy was kept at approximately 100 nJ for 2PA. A Gaussian beam profile was obtained by spatial filtering the excitation beam before the Z-scan setup. A silicon detector was employed to monitor the laser beam intensity in the far-field. To improve the signal to noise ratio, a lock-in amplifier was used to integrate 1000 shots for each point of the Z-scan signature. For nonlinear measurements, the samples were prepared in a concentration of 1 x 10^{-3} M and placed in a 2 mm fused silica cell. For an absorptive non-linearity, the light field induces an intensity dependent absorption, $\alpha = \alpha_0 + \beta I$, in which I is the laser beam intensity, α_0 is the linear absorption coefficient and β is the 2PA coefficient. Therefore, once an open aperture measurement is carried out, the nonlinear absorption coefficient can be unambiguously determined by fitting the experimental data. The two-photon absorption cross-section can be

obtained through the expression $\sigma_{2PA} = h\nu\beta/N$, where N is the number of molecules per cm^3, and *hν* is the photon energy.

C – FEMTOSECOND PUMP-PROBE MEASUREMENTS:

Femtosecond time-resolved ESA experiment was implemented using 160-fs pulses (775 nm) from a regenerative Ti:sapphire CPA (Chirped Pulse Amplifier) system operating at 1 kHz repetition rate (Clark 2001-MXR). A 90/10 beam-splitter was used to divide the beam into pump and probe pulses. The stronger beam was doubled (387.5 nm) using a 300 μm thick BBO crystal cut for type-I second harmonic generation. 1PA induced ESA measurements were performed using the pulse at 387.5 nm as pump pulse after the reminiscent fundamental beam is filtered by dichroic mirrors. For 2PA induced ESA measurements, the fundamental pulse at 775 nm was used as pump pulse. A small portion of the weaker beam was focused with a 50 mm focal length lens in a 1-mm-thick sapphire plate to generate the white-light continuum (WLC) probe. The fundamental beam intensity used to generate the WLC was carefully controlled adjusting the angle between two thin wire grid polarizers in order to achieve a stable WLC. Time-resolved ESA measurements were performed monitoring the probe intensity spectral distribution as a function of the time delay τ between pump and probe pulses, which was varied by a computer controlled translation stage that provides a resolution of 75 fs. For each time delay, the probe pulse intensity spectral distribution is recorded with and without the pump pulse irradiating the sample. In this way, we can calculate the spectra of differential absorbance (time-resolved ESA signal), $\Delta A(\lambda, \tau)$, and separate the signal related to the excited states or photo-induced species from the ground state signal. The differential absorbance signal is described by Eq.(1):

$$\Delta A(\lambda, \tau) = \frac{I_{probe}^{pump\ on}(\lambda,\tau)}{I_{probe}^{pump\ off}(\lambda,\tau)}, \qquad (1)$$

in which, $I_{probe}^{pump\ on}$ and $I_{probe}^{pump\ off}$ correspond, respectively, to the probe pulse spectra with and without the pump pulse irradiating the sample for each time delay τ. The WLC probe pulse intensity spectral distribution was monitored by means of a fast spectrometer (Ocean Optics - USB2000). The chirp of WLC probe pulse was measured to be < 1 ps in the 400-700 nm spectral region. Pump and probe pulses energies were adjusted to be smaller than 1 μJ

and 1nJ, respectively, and their polarizations relative angle was set to the magic angle (54.7^{o}) to eliminate orientational components from the signal.

III – RESULTS AND DISCUSSIONS

Figure 2 presents the normalized linear absorption (solid line) and excitation fluorescence anisotropy (diamonds) spectra of the **ATRA** in DMSO. The lowest energy one-photon allowed absorption band located at 358 nm for the **ATRA** dissolved in DMSO is related to their charge distribution along the polyene chain (1^1Ag-like→2^1Bu-like transition) [31]. Such band exhibits a considerable molar absorptivity of c.a. 2.80 ± 0.20 x 10^4 $M^{-1}cm^{-1}$ at 358 nm, which is related to the significant numbers of π-electron and planarity of polyene chain [24, 32]. The diamonds represents the excitation anisotropy spectrum. As it can be seen between 400 and 335 nm, a constant value on the excitation anisotropy is attributed to transition from the ground-state to the first strongly 1PA allowed singlet excited state (1^1Ag^--like→1^1Bu^+-like). At 290 nm, a great change in the excitation anisotropy value indicates that the angle between the absorption and emission transitions is being altered and, as consequence, another excited state should is being reached (most probably, this state is related with the 1^1Ag-like→2^1Bu^+-like transition) [33].

The 2PA cross-section spectrum for the **ATRA** in DMSO is depicted in Fig. 3 (diamonds), which was determined by performing open-aperture Z-scan measurements (the 2PA cross-section were plotted as a function of half excitation wavelength). The 2PA spectrum presents two 2PA allowed bands located at 280 nm (2hν = 560 nm) and 365 nm (2hν = 730 nm) with 2PA cross-section values of about 34 GM and 40 GM, respectively. The relatively small 2PA cross-section values observed for ATRA are probably related to the weak push-pull character of the chromophore. In fact, the β-ionone ring and carboxylic acid are, respectively, weak electron donor and moderated acceptor groups, and, therefore, the charge redistribution along the polyene chain is small at the excited state [22, 34]. In the same figure, we present the 1PA spectrum to allow a direct comparison between the energy levels involved in 1PA and 2PA allowed bands. One can observe that the 2PA band is red-shifted by approximately 7 nm in comparison to the 1PA band, indicating that the state accessed by 2PA does not correspond, necessarily, to the state accessed by one-photon. As previously reported, some studies have shown this same behavior for another retynil polyene, in special, for the all-trans retinal [24, 32, 35-38].

For molecules such as **ATRA**, in which it is not possible to define precisely the parity of excited states because of the low molecular symmetry, the same electronic state may be accessed via one and two-photon absorptions. Therefore, the 1^1Ag^--like$\rightarrow 1^1Bu^+$-like transition should contribute to the lowest-energy allowed 2PA band. In order to quantify this contribution, we performed Stokes-shift solvatochromic measurements and sum-over-essential states approach. For the lowest energy 2PA band at 730 nm (2 hv), we assumed a two-energy level system. Taking into account the average over all possible molecular orientations in an isotropic medium and considering excitation with linearly polarized light, the 2PA cross-section can be written as:

$$\sigma_{01}^{(2PA)}(\omega) = 2\frac{(2\pi)^5}{(nhc)^2}\left(\frac{2\cos^2(\theta)+1}{15}\right)L^4\left|\vec{\mu}_{01}\right|^2\left|\Delta\vec{\mu}_{01}\right|^2 g_{01}(2\omega), \quad (2)$$

in which

$$\left|\vec{\mu}_{01}\right|^2 = \frac{3\times 10^3 \ln(10)hc}{(2\pi)^2 N_A}\frac{n}{L^2}\frac{1}{\omega_{01}}\int_{\omega_1}^{\omega_2}\varepsilon(\omega)\,d\omega \quad (3)$$

and

$$\left|\Delta\vec{\mu}_{01}\right|^2 = \frac{3}{4\pi}hc\frac{\partial\upsilon}{\partial F}vol \quad (4)$$

In these equations, c is the speed of light, ω_{01} is the transition angular frequency, and $L = 3n^2/(2n^2+1)$ is the Onsager local field factor introduced to take into account the medium effect [39] with the refractive index $n=1.479$ for DMSO at 20°C. $\vec{\mu}_{01}$ is the transition dipole moment, $\Delta\vec{\mu}_{01}$ is the difference between the permanent dipole moments vectors of the excited ($\vec{\mu}_{11}$) and ground ($\vec{\mu}_{00}$) states, and θ is the angle between the dipole moments $\vec{\mu}_{01}$ and $\Delta\vec{\mu}_{01}$. By measuring the 2PA with linearly and circularly polarized light [40], we determined that $\theta \approx 0^o$. N_A is the Avogrado's number, and $g_{gf}(2\omega) = (1/\pi)\left\{\Gamma_{gf}/\left[\left(\omega_{gf}-2\omega\right)^2+\Gamma_{gf}^2\right]\right\}$ represents the normalized linewidth function (Lorentzian line-shape), in which, Γ_{gf} is the damping constant describing half width at half-maximum (FHWM) of the final state linewidth. $\upsilon = \upsilon_{abs} - \upsilon_{em}$ is the difference between the peak of the absorption and fluorescence emission in cm^{-1}.

$F(n,\xi) = 2\left[(\xi-1)/(2\xi+1) - (n^2-1)/(2n^2+1)\right]$ is the Onsager polarity function, in which, ξ is the dielectric constant of the solvent. *Vol* is the volume of the molecular cavity. To find the molecular cavity volume, we performed quantum chemical calculations based on the Density Function Theory, taken into account the DMSO solvent effect by using the Polarization Continuum Model within the integral equation formalism variant (IEF-PCM)[41]. This model is based on creating the solute cavity within the dielectric continuum via a set of overlapping spheres centered on the heavy atoms of the molecule (solute) [41]. With such approach, we determined a hydrodynamics volume for **ATRA** of approximately 515.4 Å^3.

Figure 4 (a) shows the steady-state absorption and fluorescence spectra of the **ATRA** in five different solvents (toluene, chloroform, THF, DMSO and ethanol), while Fig. 4 (b) illustrates the result of the Stokes-shift (υ) as a function of the Onsager polarity parameter ($F(n,\xi)$). We calculated a positive linear slope ($\frac{\partial \upsilon}{\partial F} = 2068 \pm 750\ \text{cm}^{-1}$), indicating that the permanent dipole moment for the first excited state is higher than the ground-state one ($\vec{\mu}_{11} > \vec{\mu}_{00}$) [42].

Using this result, the hydrodynamic volume calculated through DFT-PCM calculations and Eq. (2), we obtained a maximum 2PA cross-section of 20 ± 7 GM for the lowest energy 2PA allowed band of **ATRA** in DMSO, which is approximately half of the value experimentally observed. Using Eq. (2), we simulated the contribution of this state to the lowest-energy 2PA band as shown in Fig. 3 (black shadow Lorentzian curve). Since considering only the $1^1A_g^-$ -like $\rightarrow 1^1B_u^+$-like transition, we could not observe a good agreement between the experimental and theoretical result. This important outcome indicates that another state, which is not observed in the 1PA spectrum, is contributing to the lowest-energy 2PA band. As previously mentioned, the retinyl polyenes present two main low-lying excited singlet states, named $^1A_g^-$ -like and $^1B_u^+$-like respectively. The $1^1B_u^+$-like state is the one responsible for the considerable molar absorptivity (2.80 ± 0.10 x 10^4 $M^{-1}cm^{-1}$) at 358 nm, and, therefore, it is the state that presents 2PA cross-section of about 20 GM. In this context, the $2^1A_g^-$ -like state, which presents the same parity of the ground state ($1^1A_g^-$ -like) of retinyl polyenes, should contribute to the lowest-energy 2PA band observed in Fig. 3. We have used an analogous equation as Eq. (2) to adequately fit the experimental 2PA data. The red shaded Lorentzian curve shows the effective contribution of the $2^1A_g^-$ -like state to the lowest energy band of **ATAR** in DMSO. By integrating the Lorentzian curves, we found that

the $1^1B_u^+$-like and 2^1Ag^- -like states contribute, respectively, with 48 % and 52 % to the lowest energy 2PA band.

To shed more light about the electronic structure of **ATRA**, in special to the $2^1A_g^-$like state, we have measured the excited-state absorption for **ATRA** in DMSO solution by using the white-light femtosecond pump-probe technique. This experiment was performed in order to observe if there is or not a significant difference between the relaxation times from the both involved 2PA states to the ground state. Figure 5 shows the results of transient absorption for **ATRA** in DMSO with the pump at 387.5 nm (1PA – Fig. 5 (a)) and 775 nm (2PA – Fig. 5 (b)). In this figure, the left hand side shows the colormap representing the time- and wavelength-resolved dynamics of transient absorption spectrum; the central part displays the ESA spectra for different times, while the right hand side illustrates the decay curves for probe pulse at 540 nm (a) and 545.5 nm (b), corresponding respectively, to the peak of the 1PA and 2PA ESA spectra.

The inset in Figs. 5 (right side) depicts the decay time as a function of the excitation wavelength. As can be seen in Fig. 5, the spectral and temporal dynamics can be considered the same, given our experimental error, for **ATRA** when excited by one- or two-photon absorption.

More specifically, when **ATRA** is excited by one-photon (387.5 nm), we observed an electronic relaxation time of approximately 3.2 ps at 540 nm (ESA-1PA peak). For the probe at 545.5 nm (ESA-2PA peak), when the sample is excited by two-photon of 775 nm the electronic relaxation time is 3.3 ps. The difference observed between the 1PA and 2PA excited decay curves for **ATRA** are within the experimental error (laser pulse with FWHM linewidth of ~ 160 fs). In Fig. 6 we show a comparison between the ESA spectra for the pump laser at 387.5 nm (1PA) and 775 nm (2PA).

It is observed in Fig. 6 that the ESA spectrum excited by 2PA present a red-shift of *c.a.* 5.5 nm when compared to the ESA spectrum excited by 1PA. This result indicates the pump pulses, which have the same total energy (one photon of 387.5 nm and two photons of 775 nm have energy of about 3.18 eV), promote electrons to different energy levels, analogously to what was observed in Fig. 3. This result indicates that although the pump pulses at 387.5 nm and 775 nm induces transitions at the same total energy (~ 3.18 eV), by 1PA and 2PA respectively, they promote electrons to different electronic states whose central energy are slightly displaced, analogously to what was observed in Fig. 3.

Finally, in order to model the higher energy 2PA allowed band at 280 nm (see Fig. 3), we used a three-level energy diagram, consisting of a ground-state (1^1Ag^- -like), one

intermediate 1PA allowed excited state ($1^1B_u^+$-like) and the final excited state ($\left|S_f\right\rangle$). For this system, the 2PA cross-section can be written as (assuming linearly polarized light and that the dipole moments are parallel): [40]

$$\sigma_{0f}^{(2PA)}(\omega) = \frac{2}{5}\frac{(2\pi)^5}{(nhc)^2} L^4 R(\omega) \left|\vec{\mu}_{01}\right|^2 \left|\vec{\mu}_{1f}\right|^2 g_{0f}(2\omega), \quad (5),$$

in which, $\vec{\mu}_{12}$ is the transition dipole moment between the excited states $\left|S_1\right\rangle \rightarrow \left|S_f\right\rangle$, and $R(\omega) = \omega^2 \Big/ \left[(\omega_{01} - \omega)^2 + \Gamma_{01}^2(\omega)\right]$ is the resonance enhancement factor. In general, for non-centrosymmetric molecules as **ATRA**, Eq. (5) presents additional terms related with the permanent dipole moment change and the interference term between the two distinct excitation channels.[40] However, in molecular system with a weak push-pull character as observed in **ATRA**, the factor $R(\omega)\left|\vec{\mu}_{01}\right|^2 \left|\vec{\mu}_{1f}\right|^2$ dominates the 2PA allowed transition. Considering the experimental data obtained from the Z-scan measurements at 280 nm (2ν = 560 nm), $\sigma^{(2PA-\max)} = 34\ GM$, we found $\left|\vec{\mu}_{1f_1}\right| = 5.5D$. Such value corresponds to a molar absorptivity of approximately 1.74 x 10^4 $M^{-1}cm^{-1}$. In order to observe this band along the ESA, it is necessary to use a probe with wavelength higher than 850 nm. However, in our experiment, the filter used to remove the strong 775 nm that generates the white-light probe pulses also remove wavelengths longer than 770 nm. In addition, as the molar absorptivity to this transition is smaller than those to the ground state, this region should be associated with the saturable absorption effect [43]. However, to the resonance enhancement effect region (shorter than 280 nm, data not shown), we observed a 2PA cross-section about 140 GM (at 250 nm or 2ν = 500 nm), which, using Eq. (5), gives a $\left|\vec{\mu}_{1f_2}\right| = 12.0D$. Such value corresponds to a molar absorptivity of ~ 9.5 x 10^4 $M^{-1}cm^{-1}$, which is similar to the one estimated for the **ATRA** (~ 1.25 x 10^5 $M^{-1}cm^{-1}$ at 540 nm) using rhodamine B as reference material [44] through the pump-probe experiments [45]. This result indicates that the same states are being accessed by one- and two-photon absorption at the resonance enhancement region.

4– FINAL REMARKS

In this study we have investigated the 2PA spectrum of **ATRA**, a chromophore with interesting optical and biological properties, by using the steady and transient 2PA spectroscopy. We observed that **ATRA** presents a 2PA spectrum composed by a 2PA band of high energy (280 nm) that has contribution of an intermediate excited state and a lowest-energy 2PA band. The latter band was ascribed to the overlap between the 2^1Ag-like and 1^1Bu-like states due the lower molecular symmetry of the **ATRA**, which allows electrons to be excited by 2PA to states with different parity in respect to the ground state. By means of solvatochromic measurements and using a two-energy level model, we were able to quantify the individual contribution of the 2^1Ag-like and 1^1Bu-like states to the lowest energy 2PA band. We found similar behavior between the 2PA and ESA-2PA spectra as compared to their correspondent 1PA and ESA-1PA spectra, more specifically, a red-shift of about 5.5 nm was observed to the 2PA spectra. In summary, here we reported for the first time the 2PA cross-section spectrum and the excited state dynamic induced by 2PA for the **ATRA** dissolved in DMSO. We believe that these results contribute to a better understanding of the photochemical and nonlinear optical features of polyenes as **ATRA**.

ACKNOWLEDGMENTS

Financial support from FAPESP (Fundação de Amparo à Pesquisa do estado de São Paulo, processo n°: 2011/12399-0 and n°: 2009/11810-8), FAPEMIG (Fundação de Amparo à Pesquisa do estado de Minas Gerais), CNPq (Conselho Nacional de Desenvolvimento Científico e Tecnológico), CAPES (Coordenação de Aperfeiçoamento de Pessoal de Nível Superior) and the Air Force Office of Scientific Research (FA9550-12-1-0028) are acknowledged.

REFERENCES

(1) Birge, R. R., Photophysics and molecular electronic applications of the rhodopsins. *Annu Rev Phys Chem* 1990, **41**, 683-733.

(2) Birge, R. R.; Knox, B. E., Perspectives on the counterion switch-induced photoactivation of the G protein-coupled receptor rhodopsin. *P Natl Acad Sci USA* 2003, **100**, 9105-9107.

(3) Birge, R. R.; Gillespie, N. B.; Izaguirre, E. W.; Kusnetzow, A.; Lawrence, A. F.; Singh, D.; Song, Q. W.; Schmidt, E.; Stuart, J. A.; Seetharaman, S.; Wise, K. J., Biomolecular

electronics: Protein-based associative processors and volumetric memories. *J Phys Chem B* 1999, **103**, 10746-10766.

(4) Zhang, T. H.; Zhang, C. P.; Fu, G. H.; Li, Y. D.; Gu, L. Q.; Zhang, G. Y.; Song, Q. W.; Parsons, B.; Birge, R. R., All-optical logic gates using bacteriorhodopsin films. *Opt Eng* 2000, **39**, 527-534.

(5) Roy, S.; Prasad, M.; Topolancik, J.; Vollmer, F., All-optical switching with bacteriorhodopsin protein coated microcavities and its application to low power computing circuits. *J Appl Phys* 2010, **107**.

(6) Koyama, Y., Structures and functions of carotenoids in photosynthetic systems. *J Photoch Photobio B* 1991, **9**, 265-280.

(7) Krueger, B. P.; Scholes, G. D.; Jimenez, R.; Fleming, G. R., Electronic excitation transfer from carotenoid to bacteriochlorophyll in the purple bacterium Rhodopseudomonas acidophila. *J Phys Chem B* 1998, **102**, 2284-2292.

(8) Berera, R.; van Grondelle, R.; Kennis, J. T. M., Ultrafast transient absorption spectroscopy: principles and application to photosynthetic systems. *Photosynth Research* 2009, **101**, 105-118.

(9) Thompson, M.; Williams, C. R., Stability of flavonoid complexes of copper(II) and flavonoid antioxidant activity. *Anal Chim Acta* 1976, **85**, 375-381.

(10) Torel, J.; Cillard, J.; Cillard, P., Antioxidant activity of flavonoids and reactivity with peroxy radical. *Phytochem* 1986, **25**, 383-385.

(11) Lekka, C. E.; Ren, J.; Meng, S.; Kaxiras, E., Structural, Electronic, and Optical Properties of Representative Cu-Flavonoid Complexes. *J Phys Chem B* 2009, **113**, 6478-6483.

(12) Birge, R. R., Photophysics of light transduction in rhodopsin and bacteriorhodopsin. *Ann Rev Biophys Bioeng* 1981, **10**, 315-354.

(13) Birge, R. R.; Hubbard, L. M., Molecular-dynamics of cis-trans isomerization in rhodopsin. *J Am Chem Soc* 1980, **102**, 2195-2205.

(14) Birge, R. R.; Einterz, C. M.; Knapp, H. M.; Murray, L. P., The nature of the primary photochemical events in rhodopsin and isorhodopsin. *Biophys J* 1988, **53**, 367-385.

(15) Birge, R. R.; Murray, L. P.; Pierce, B. M.; Akita, H.; Baloghnair, V.; Findsen, L. A.; Nakanishi, K., 2-Photon spectroscopy of locked-11-cis-rhodopsin - evidence for a protonated schiff-base in a neutral protein-binding site. *P Natl Acad Sci USA* 1985, **82**, 4117-4121.

(16) Gai, F.; Hasson, K. C.; McDonald, J. C.; Anfinrud, P. A., Chemical Dynamics in Proteins: The Photoisomerization of Retinal in Bacteriorhodopsin. *Science* 1998, **279**, 1886-1891.

(17) Kobayashi, T.; Saito, T.; Ohtani, H., Real-time spectroscopy of transition states in bacteriorhodopsin during retinal isomerization. *Nature* 2001, **414**, 531-534.

(18) Polli, D.; Altoe, P.; Weingart, O.; Spillane, K. M.; Manzoni, C.; Brida, D.; Tomasello, G.; Orlandi, G.; Kukura, P.; Mathies, R. A.; Garavelli, M.; Cerullo, G., Conical intersection dynamics of the primary photoisomerization event in vision. *Nature* 2010, **467**, 440-U88.

(19) Minucci, S.; Leid, M.; Toyama, R.; SaintJeannet, J. P.; Peterson, V. J.; Horn, V.; Ishmael, J. E.; Bhattacharyya, N.; Dey, A.; Dawid, I. B.; Ozato, K., Retinoid X receptor (RXR) within the RXR-retinoic acid receptor heterodimer binds its ligand and enhances retinoid-dependent gene expression. *Mol Cell Bio* 1997, **17**, 644-655.

(20) Szuts, E. Z.; Harosi, F. I., Solubility of retinoids in water. *Arch Biochem Biophys* 1991, **287**, 297-304.

(21) Zanotti, G.; Dacunto, M. R.; Malpeli, G.; Folli, C.; Berni, R., Crystal-structure of the transthyretin retinoic-acid complex. *Eur J Biochem* 1995, **234**, 563-569.

(22) Sporn, M. B.; Roberts, A. B.; Goodman, D. S., *The Retinoids*. Academic Press: 1984; Vol. 1.

(23) Birge, R. R.; Bennett, J. A.; Hubbard, L. M.; Fang, H. L.; Pierce, B. M.; Kliger, D. S.; Leroi, G. E., Two-photon spectroscopy of all-trans-retinal. Nature of the low-lying singlet states. *J Am Chem Soc* 1982, **104**, 2519-2525.

(24) Birge, R. R.; Pierce, B. M., A Theoretical analysis of the two-photon properties of linear polyenes and the visual chromophores. *J Chem Phys* 1979, **70**, 165-178.

(25) Hudson, B.; Kohler, B., Linear polyene electronic-structure and spectroscopy. *Ann Rev Phys Chem* 1974, **25**, 437-460.

(26) Yamaguchi, S.; Tahara, T., Two-photon absorption spectrum of all-trans retinal. *J Chem Phys Lett* 2003, **376**, 237-243.

(27) Presiado, I.; Shomer, S.; Erez, Y.; Gepshtein, R.; Amdursky, N.; Huppert, D., Time-resolved emission of retinoic acid. *J Photoch Photobio A* 2013, **258**, 30-40.

(28) Zhang, L.; Yang, J.; Wang, L.; Yang, G. Z.; Weng, Y. X., Direct observation of interfacial charge recombination to the excited-triplet state in all-trans-retinoic acid sensitized TiO2 nanoparticles by femtosecond time-resolved difference absorption spectroscopy. *J. Phys Chem B* **2003,** 107, 13688-13697.

(29) Polivka, T.; Sundstrom, V., Dark excited states of carotenoids: Consensus and controversy. *Chem Phys Lett* **2009,** 477, 1-11.

(30) Ostroumov, E. E.; Mulvaney, R. M.; Cogdell, R. J.; Scholes, G. D., Broadband 2D Electronic Spectroscopy Reveals a Carotenoid Dark State in Purple Bacteria. *Science* **2013,** 340, 52-56.

(31) Vivas, M. G., Silva, D. L., Misoguti, L., Zalesny, R., Bartkowiak, W., Mendonca, C. R., Degenerate Two-Photon Absorption in All-Trans Retinal: Nonlinear Spectrum and Theoretical Calculations. *J Phys Chem A* 2010, **114**, 3466–3470.

(32) Hudson, B. S.; Kohler, B. E., Linear polyene electronic structure and spectroscopy. *Chem Phys Lett* 1972, **14**, 299-304.

(33) Lakowicz, J. R., *Principles of Fluorescence Spectroscopy*. Springer 2006; p 954.

(34) Marder, S. R.; Sohn, J. E.; Stucky, G. D., *Materials for Nonlinear Optics*. American Chemical Society: 1991; **455**.

(35) Hudson, B. S.; Kohler, B. E., Polyene Spectroscopy - Lowest Energy Excited Singlet-State of Diphenyloctatetraene and Other Linear Polyenes. *J Chem Phys* 1973, **59**, 4984-5002.

(36) Vivas, M. G.; Silva, D. L.; de Boni, L.; Zalesny, R.; Bartkowiak, W.; Mendonca, C. R., Two-photon absorption spectra of carotenoids compounds. *J Appl Phys* 2011, **109**.

(37) Larson, E. J.; Friesen, L. A.; Johnson, C. K., An ultrafast one-photon and two-photon transient absorption study of the solvent-dependent photophysics in all-trans retinal. *Chem Phys Lett* 1997, **265**, 161-168.

(38) Merchán, M.; González-Luque, R., Ab initio study on the low-lying excited states of retinal. *J Chem Phys* 1996, **106**, 1112-1222.

(39) Onsager, L., Electric moments of molecules in liquids. *J Am Chem Soc* 1936, **58**, 1486-1493.

(40) Vivas, M. G.; Silva, D. L.; De Boni, L.; Bretonniere, Y.; Andraud, C.; Laibe-Darbour, F.; Mulatier, J. C.; Zalesny, R.; Bartkowiak, W.; Canuto, S., Revealing the Electronic and Molecular Structure of Randomly Oriented Molecules by Polarized Two-Photon Spectroscopy. *J. Phys. Chem. Lett* 2013, **4**, 1753-1759.

(41) Tomasi, J.; Mennucci, B.; Cances, E., The IEF version of the PCM solvation method: an overview of a new method addressed to study molecular solutes at the QM ab initio level. *J Mol Struct-Theochem* 1999, **464**, 211-226.

(42) Reichardt, C., Solvatochromic dyes as solvent polarity indicators. *Chem Rev* 1994, **94**, 2319-2358.

(43) Perry, J. W.; Mansour, K.; Marder, S. R.; Perry, K. J.; Alvarez, D.; Choong, I., Enhanced reverse saturable absorption and optical limiting in heavy-atom-substituted phthalocyanines. *Opt Lett* 1994, **19**, 625-627.

(44) Beaumont, P. C.; Johnson, D. G.; Parsons, B. J., Photophysical properties of laser-dyes - picosecond laser flash-photolysis studies of rhodamine-6G, rhodamine-b and rhodamine-101. *J Chem Soc-Farad T* 1993, **89**, 4185-4191.

(45) Cui, L. Nonlinear Imaging in Scattering Media with Pump-probe and Fluorescence based Techniques. University of Rochester, 2011.

Figure captions

Figure 1 – Chemical structure for the all-trans retinoic acid.

Figure 2 – Ground-state (solid line – left axis) and excitation fluorescence anisotropy (diamonds, right axis) spectra of **ATRA** dissolved in DMSO at room temperature.

Figure 3 –The black solid line represent the 1PA spectrum, while the diamonds represent the 2PA spectrum of **ATRA** dissolved in DMSO at room temperature. The shades curves represent the individual contribution to the lowest energy 2PA band of the 2^1Ag-like and 1^1Bu-like states found in this study. The red line along the diamonds represents the sum of both individual contributions.

Figure 4 – (a) Normalized absorption and fluorescence spectra for **ATRA** in five different solvents (toluene, chloroform, dichloromethane, THF, DMSO and ethanol). (b) Solvatochromic Stokes shift (υ) measurements obtained as a function of the Onsager polarity function ($F\left(n,\xi\right)$).

Figure 5 –Excited state dynamics for **ATRA** in DMSO solution (a) 1PA and (b) 2PA excitations. ESA colormap representing the time- and wavelength-resolved dynamics of transient absorption spectrum (left hand). ESA spectra for different times (central part). Decay curves for probe pulse at (a) 540 nm and 545.5 nm (b) corresponding, respectively, to the 1PA and 2PA ESA peak (right hand).

Figure 6 –Comparison between the ESA spectra excited by one- and two-photon absorption. It is observed a red-shift to the ESA spectrum excited by two-photons (775 nm) in comparison to the one-photon excited one (387.5 nm). Both curves correspond to the same time.

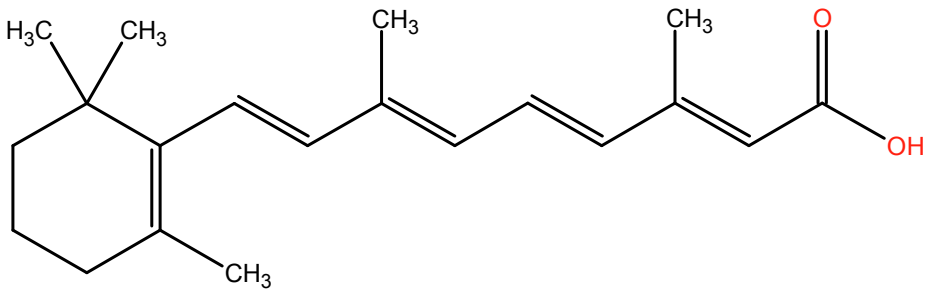

Figure 1

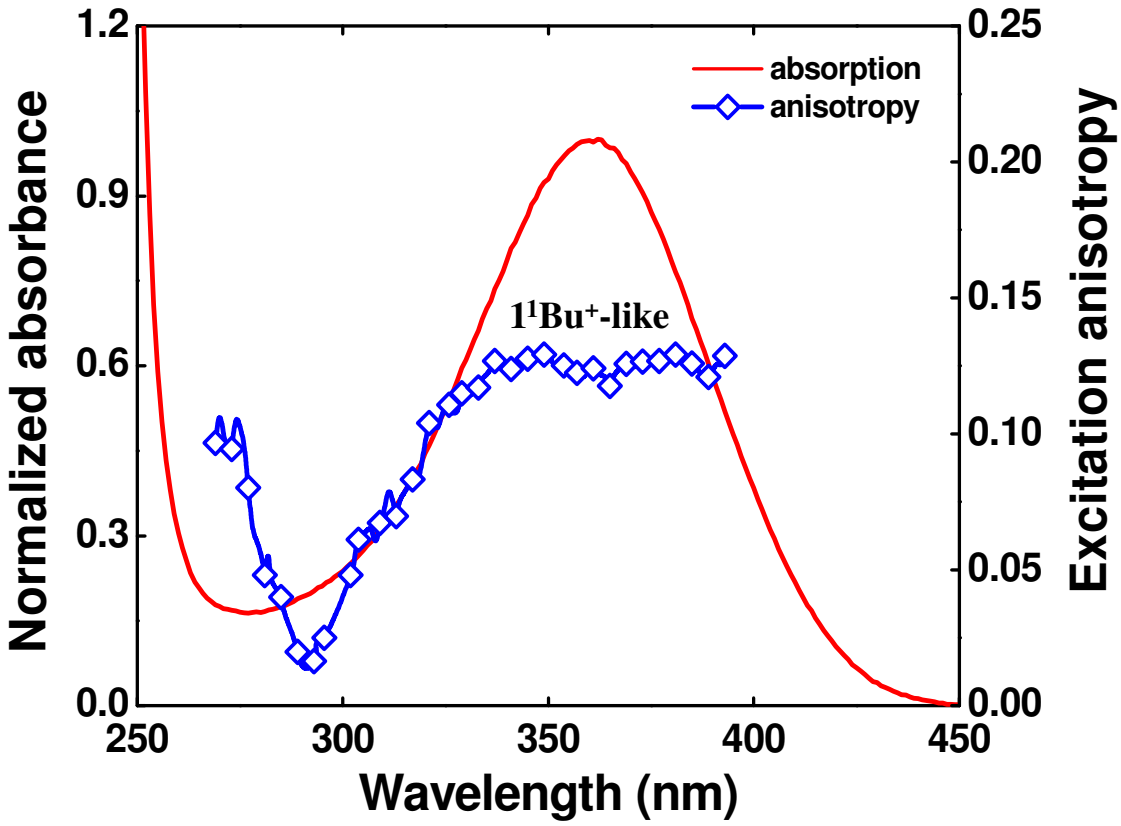

Figure 2

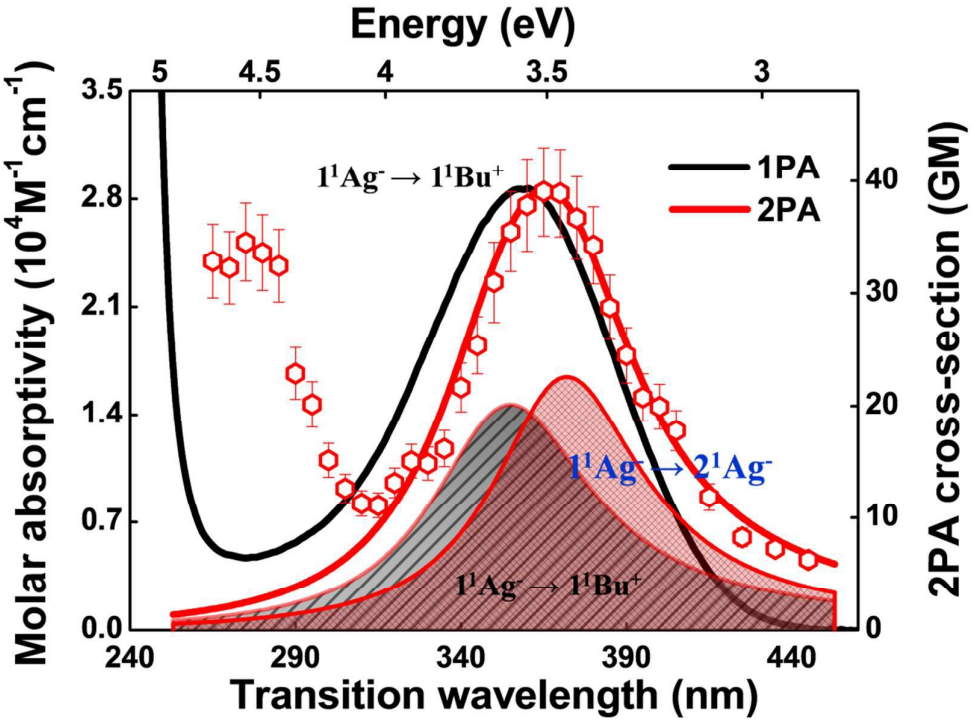

Figure 3

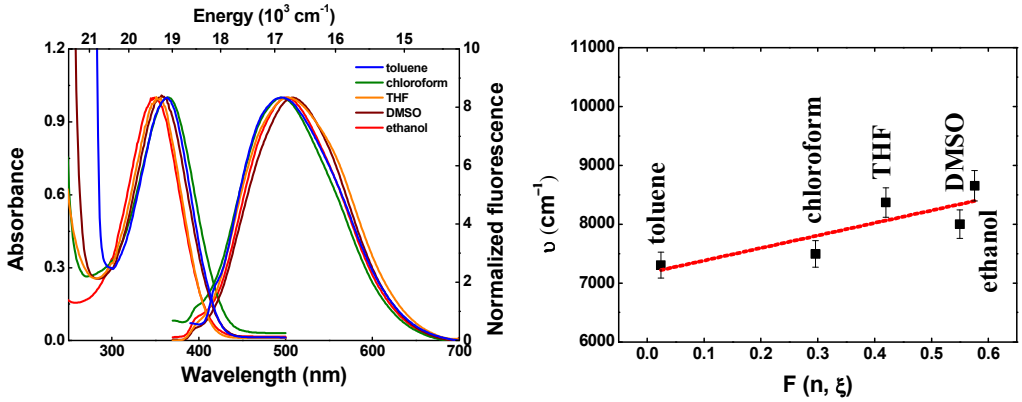

Figure 4

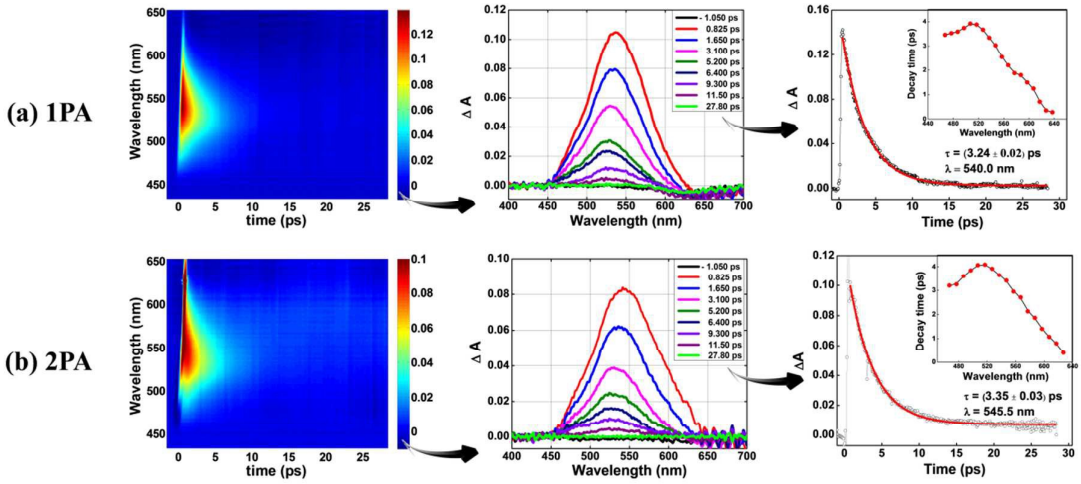

Figure 5

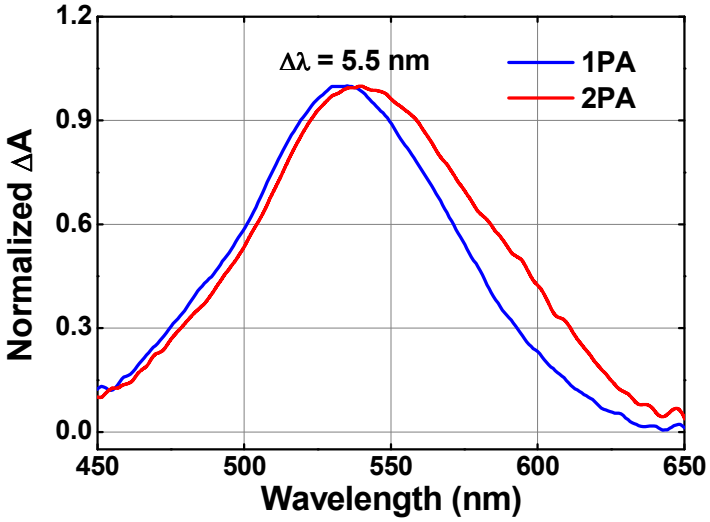

Figure 6

Table of Contents – Graphic

This paper reports for the first time a complete study on the steady and transient excited state dynamics induced by 2PA for **ATRA**.